INTERNATIONAL JOURNAL FOR NUMERICAL METHODS IN FLUIDS, VOL. 9, 1059–1072 (1989)

FINITE ELEMENT TECHNIQUE TO SOLVE THE ELASTIC STRAIN FOR LEONOV FLUID FLOW

GWO-GENG LIN

Department of Chemical Engineering, Tamkang University, Tamsui, Taiwan, R.O.C.

HSIENG-CHENG TSENG* AND YI-SHI JU

Department of Chemical Engineering, National Taiwan Institute of Technology, Taipei, R.O.C.

SUMMARY

The finite element method is used to find the elastic strain (and thus the stress) for given velocity fields of the Leonov model fluid. With a simple linearization technique and the Galerkin formulation, the quasi-linear coupled first-order hyperbolic differential equations together with a non-linear equality constraint are solved over the entire domain based on a weighted residual scheme. The proposed numerical scheme has yielded efficient and accurate convective integrations for both the planar channel and the diverging radial flows for the Leonov model fluid. Only the strain in the inflow plane is required to be prescribed as the boundary conditions. In application, it can be conveniently incorporated in an existing finite element algorithm to simulate the Leonov viscoelastic fluid flow with more complex geometry in which the velocity field is not known *a priori* and an iterative procedure is needed.

KEY WORDS Viscoelastic flow Leonov model Convective integration Finite element method

INTRODUCTION

Numerical simulation of viscoelastic flows has been at the forefront of research in the area of rheology for quite some time. For a successful simulation, one needs a constitutive equation which can predict different viscoelastic phenomena for a range of materials, and a numerical scheme which is capable of handling the resulting equations. Most of the theoretical works devoted to the entrance flow problem[1–9] have been based upon the Maxwell-type constitutive model in differential or integral forms. A very good review of works in this area was given by White *et al.*[10] They indicated that for a number of viscoelastic models, numerical calculations usually failed to converge at relatively low shear rates (with Deborah number of the order of unity). Yeh[6] categorized the possible causes for the numerical difficulties into five classes: instability of the weighted residual method, poor approximation to the steep stress gradients, geometrical singularity, multiplicity or loss of solution, and changing the type of system of equations from elliptic to hyperbolic. Crochet *et al.*[11] reached almost the same conclusions in their book. In addition, they recognized that minor changes in the constitutive equation and/or the algorithm employed can lead to higher limiting values of We or S_R. Recently, the Leonov model[12,13] was used to simulate the polymeric flow with critical Deborah numbers up to 100[14] and 50.[15]

* Author to whom all correspondence should be addressed.

0271–2091/89/091059–14$07.00

Received June 1988
Revised 8 September 1988

The Leonov model has been employed in many investigations[16-18] under different flow situations and found to have good predictive capability and also to be quite readily amenable to numerical implementation. In Reference 15 the Leonov constitutive equation has been applied to two-dimensional flow simulation and a relaxation factor was used in the momentum equation, with the stresses being evaluated via a streamwise integration procedure following the general approach of Viryayuthakorn and Caswell.[4] The convergence of the numerical scheme has been tested on a 2:1 abrupt contraction flow problem by successive mesh refinement for non-dimensional characteristic shear rates of 5 and 50 for polyisobutylene Vistanex at 27 °C.

The streamline integration technique requires separate algorithms for locating the streamline and integrating the evolution equations. As the number of dimensions in the formulation is increased, the complexity of evaluating the streamline position increases. To trace a particle path that is very close to a surface is difficult for the streamline technique. The accumulation of small errors in definining the streamline position may result in the particle crossing the element boundary at the wrong point and therefore lead to an erroneous final strain.[23] Viryayuthakorn and Caswell[4] also reported that the real limitation on the streamline integration appears to be the spatial interpolation of the displacement field. Especially as the Deborah number is increased, even larger displacements must be tracked and the assumed element displacement field becomes inaccurate.

On the other hand, numerical implementation of the integration by the finite element method is very straightforward. This is especially true when the integration of the strain (or other evolutionary variables) is part of a more general finite element model such as that used for the velocity field calculations. Much of the coding required to implement a Galerkin formulation is already available from the solution of the velocity field (or temperature distribution, for thermomechanically coupled problems), and only the elemental stiffness matrix is totally new. For many other evolutionary equations, the coefficient matrix obtained from the finite element formulation stems from the term involving the material derivative, which depends only on the geometry and the velocity field. Once the matrix has been assembled and triangularized, it can be used to evaluate a variety of quantities of the same order, leading to very cost-effective solutions.[19] From these points of view, the finite element formulation has advantages.

Especially, it should be noted that if the number of modes for the Leonov model is increased, the degrees of freedom could be too large to be solved for the mixed finite element formulation. In this paper we present a finite element scheme for carrying out such a convective integration in a very straightforward and efficient manner. This technique can be conveniently incorporated as an inner loop to an existing cyclic iteration algorithm[20] for the analysis of viscoelastic flows (with a wide range of constitutive models).

THE LEONOV MODEL

According to Leonov,[12] contributions to the deviatoric stress tensor $\boldsymbol{\tau}'$ due to the viscous and elastic deformations are superposed and, further, the elastic contribution is decomposed into a number of modes, for each of which, e.g. the κth mode, an elastic deformation tensor $\mathbf{C}^{(\kappa)}$ is introduced. The constitutive equation with N modes is

$$\boldsymbol{\tau}' = \eta_0 s\boldsymbol{\varepsilon} + \sum_{\kappa=1}^{N} (\eta_\kappa/\theta_\kappa)\mathbf{C}^{(\kappa)}, \tag{1}$$

where $\boldsymbol{\varepsilon}$ is the rate of deformation, η_0 is the zero-shear-rate (Newtonian) viscosity, η_κ and θ_κ are respectively the shear viscosity and relaxation time of the κth mode, and $0 < s < 1$ is a rheological

constant. The equation satisfied by $\mathbf{C}^{(\kappa)}$ is uncoupled from other modes:

$$\frac{\delta}{\delta t}\mathbf{C}^{(\kappa)} + \frac{1}{2\theta_\kappa}(\mathbf{C}^{(\kappa)}\cdot\mathbf{C}^{(\kappa)} - \mathbf{I}) = \mathbf{0}. \tag{2}$$

The convective derivative $\delta/\delta t$ is defined as

$$\frac{\delta}{\delta t}\mathbf{C} = \frac{\partial}{\partial t}\mathbf{C} + \mathbf{V}\cdot\nabla\mathbf{C} - (\nabla\mathbf{V})^{\mathrm{T}}\cdot\mathbf{C} - \mathbf{C}\cdot\nabla\mathbf{V},$$

where $\nabla\mathbf{V}$ is the gradient of the velocity field and $(\nabla\mathbf{V})^{\mathrm{T}}$ is the transpose of $\nabla\mathbf{V}$.

As the elastic effects tend to be zero in a steady flow, equation (2) gives[14]

$$\mathbf{C}^{(\kappa)} \simeq \mathbf{I} + \theta_\kappa\varepsilon. \tag{3}$$

Hence, to reproduce the Newtonian behaviour at vanishing shear rates, equation (1) requires

$$\eta_0 = \sum_{\kappa=1}^{N} \eta_\kappa(1-s)^{-1}.$$

Further, for self-consistency there is a constraint on $\mathbf{C}^{(\kappa)}$,

$$\det\mathbf{C}^{(\kappa)} = 1, \tag{4}$$

which for two-dimensional flows is simply

$$C_{11}^{(\kappa)}\cdot C_{22}^{(\kappa)} - (C_{12}^{(\kappa)})^2 = 1, \tag{5}$$

where $C_{ij}^{(\kappa)}$ denotes the ijth component of $\mathbf{C}^{(\kappa)}$. It turns out that all the material constants can be determined from standard experiments, e.g. the steady flow through a capillary rheometer or the dynamic response with oscillatory plates. As shown in References 16, 17 and 21, the Leonov model performs well in predicting the results of a host of different transient viscoelastic experiments on the basis of the constants chosen to fit standard characterization curves.

GALERKIN FORMULATION

The purpose of this paper is to present an efficient FEM scheme to integrate the Leonov constitutive equation (2) (which is a set of quasi-linear coupled first-order hyperbolic PDEs) together with a non-linear algebraic constraint (4). In this regard, focusing attention on the two-dimensional system, the governing equations based upon the Leonov model are of the component forms (assuming a known velocity field)

$$\frac{\mathrm{D}C_{11,\kappa}}{\mathrm{D}t} = 2\left(\frac{\partial u}{\partial x}C_{11,\kappa} + \frac{\partial u}{\partial y}C_{12,\kappa}\right) + \frac{1}{2\theta_\kappa}(1 - C_{11,\kappa}^2 - C_{12,\kappa}^2), \tag{6}$$

$$\frac{\mathrm{D}C_{12,\kappa}}{\mathrm{D}t} = \frac{\partial v}{\partial x}C_{11,\kappa} + \frac{\partial u}{\partial y}C_{22,\kappa} - \frac{C_{12,\kappa}}{2\theta_\kappa}(C_{11,\kappa} + C_{22,\kappa}), \tag{7}$$

$$C_{22,\kappa} = \frac{1 + C_{12,\kappa}^2}{C_{11,\kappa}}, \tag{8}$$

where $\mathrm{D}/\mathrm{D}t$ denotes the substantive time derivative $(\partial/\partial t + u\,\partial/\partial x + v\,\partial/\partial y)$.

It should be noted that the differential equation for component C_{22} is omitted and the equality constraint is incorporated instead. The elastic strain field can be found by solving equations (6),

(7) and (8). Equations (6) and (7) can be linearized and simplified as below (for the steady flow case):

$$u\frac{\partial C_{11}}{\partial x} + v\frac{\partial C_{11}}{\partial y} - 2u_x C_{11} + \frac{\hat{C}_{11}}{2\theta}C_{11} - 2u_y C_{12} + \frac{\hat{C}_{12}}{2\theta}C_{12} = \frac{1}{2\theta}, \tag{9}$$

$$-v_x C_{11} + \frac{\hat{C}_{12}}{2\theta}C_{11} + u\frac{\partial C_{12}}{\partial x} + v\frac{\partial C_{12}}{\partial y} + \frac{\hat{C}_{22}}{2\theta}C_{12} = u_y \hat{C}_{22}, \tag{10}$$

where u_x, u_y and v_x denote the spatial derivatives of velocity components u and v respectively, and $\hat{}$ denotes the value at the previous iteration step. The elastic strain tensor component C_{22} is represented by $\hat{C}_{22}$, which is evaluated from $\hat{C}_{11}$ and $\hat{C}_{12}$ via the equality constraint (8) during the iteration process, thus eliminating the equation for the C_{22} component. Because the strain tensors for the different modes are independent, the subscript κ in equations (6), (7) and (8) is neglected for convenience.

A finite element approximation for C_{11} and C_{12} can be given as

$$C_{11}(x, y) \simeq N_i C_{11i}, \qquad C_{12}(x, y) \simeq N_i C_{12i}, \tag{11}$$

where the N_i are the basis functions associated with node i, and C_{11i} and C_{12i} are the nodal values of the approximations to $C_{11}(x, y)$ and $C_{12}(x, y)$ respectively. The following compact form is then obtained from the standard Galerkin formulation:

$$\begin{bmatrix} [K1] & [K2] \\ [K3] & [K4] \end{bmatrix} \begin{Bmatrix} \{C11\} \\ \{C12\} \end{Bmatrix} = \begin{Bmatrix} \{F1\} \\ \{F2\} \end{Bmatrix}, \tag{12}$$

where

$$K1_{ij} = \int_\Omega N_i\left(u\frac{\partial N_j}{\partial x} + v\frac{\partial N_j}{\partial y} - 2u_x N_j + \frac{\hat{C}_{11}}{2\theta}N_j\right)\mathrm{d}A,$$

$$K2_{ij} = \int_\Omega N_i\left(-2u_y N_j + \frac{\hat{C}_{12}}{2\theta}N_j\right)\mathrm{d}A,$$

$$K3_{ij} = \int_\Omega N_i\left(-v_x N_j + \frac{\hat{C}_{12}}{2\theta}N_j\right)\mathrm{d}A,$$

$$K4_{ij} = \int_\Omega N_i\left(u\frac{\partial N_j}{\partial x} + v\frac{\partial N_j}{\partial y} + \frac{\hat{C}_{22}}{2\theta}N_j\right)\mathrm{d}A,$$

$$F1_i = \int_\Omega N_i\frac{1}{2\theta}\mathrm{d}A, \qquad F2_i = \int_\Omega N_i u_y \hat{C}_{22}\,\mathrm{d}A$$

and $\{C11\}$, $\{C12\}$ are the vectors of nodal values of C_{11i} and C_{12i}.

SOLUTION PROCEDURES

The nine-node quadratic rectangular element was chosen to discretize the strain field domain, and the finite element equations (12) were solved iteratively by use of an under-relaxation method with a weighting factor of 0·5 for the newly iterated values. The Newton–Raphson method was also tried but not successful. The criterion for convergence was based upon an error measure ϕ_i of

C_{11} and C_{22} from one step to the next. The error was defined, e.g. for C_{11}, as

$$\phi_i = \left| \frac{C_{11i}^{n+1} - C_{11i}^{n}}{C_{11i}^{n+1}} \right|.$$

When the maximal relative errors (over all the nodes) for both C_{11} and C_{22} were no more than 0·01, the solution was said to have converged.

TEST PROBLEMS

To illustrate the calculations of the elastic strain for the Leonov model by use of the above algorithm, we chose test problems of the straight planar channel flow and the expanding radial flow shown in Figures 1 and 2 respectively. The velocity and strain fields for both flows can be easily found, thus validating the present numerical scheme.

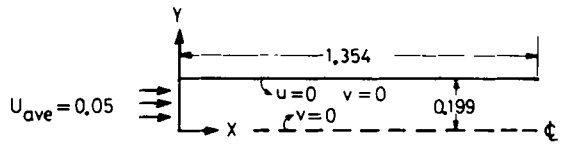

Figure 1. Schematic diagram of planar flow through a straight channel

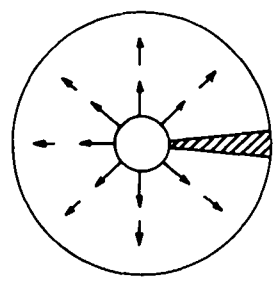

(a)

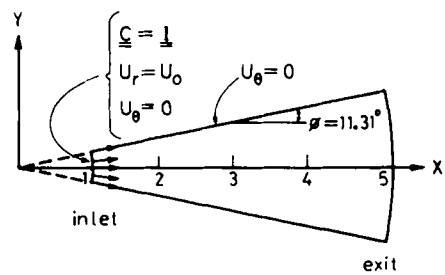

(b)

Figure 2. (a) Geometry of the diverging radial flow problem. The hatched area shows the domain for the FEM analysis. (b) Schematic diagram of the diverging flow problem which represents the hatched area of (a)

Plane channel flow

A sample calculation of fully developed flow of Leonov fluid in a planar straight channel has been carried out for polyisobutylene (Vistanex) having the following values of parameters corresponding to a two-mode fit at 27 °C:[14,15] $s = 0{\cdot}01$; $\eta_\kappa = 3{\cdot}58 \times 10^4$ and $2{\cdot}95 \times 10^4$ Pa s; $\theta_\kappa = 6{\cdot}07$ and $0{\cdot}47$ s.

The finite element mesh used for the computations is shown in Figure 3(a) with 209 nodes and 45 elements. Computations were carried out for an average velocity $U = 0{\cdot}05$, corresponding to a Deborah number of 4·6 and 0·4 based upon the wall shear rate for the two modes respectively. Material entering the region is assumed to be flowing in a fully developed (Leonov fluid flow) state. The numerical scheme was stable, with convergence being reached within 15 iteration steps for a wide range of initial guesses. Velocity and strain fields can be readily solved.[22] This analytical solution was used to compare with the FEM results. Different initial guesses were chosen for the elastic strain **C**, such as unity tensor, ten times or half of the fully developed strain, to investigate the stability and convergence of this numerical algorithm. Figure 4 shows a satisfactory agreement between the simulated and analytic solutions at the exit of the planar channel flow. Figure 5 shows excellent convergence of the scheme for the wide range of initial guesses.

Diverging radial flow

The second test problem is the calculation of the elastic strain for a one-dimensional radial flow. Material enters at the inside of an annular region and flows radially outward (Figure 2). The entering velocity is specified, which, because the material is incompressible and the flow is one-dimensional, is sufficient to define the velocity everywhere within the region. This exact velocity

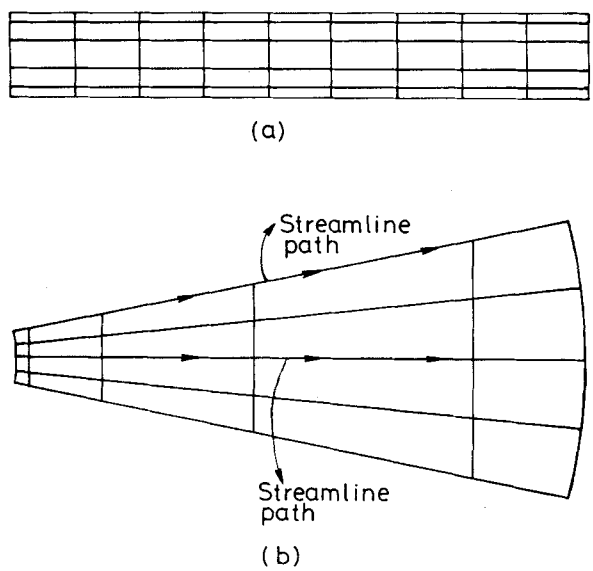

Figure 3. Finite element meshes for (a) straight planar flow and (b) diverging radial flow (mesh A)

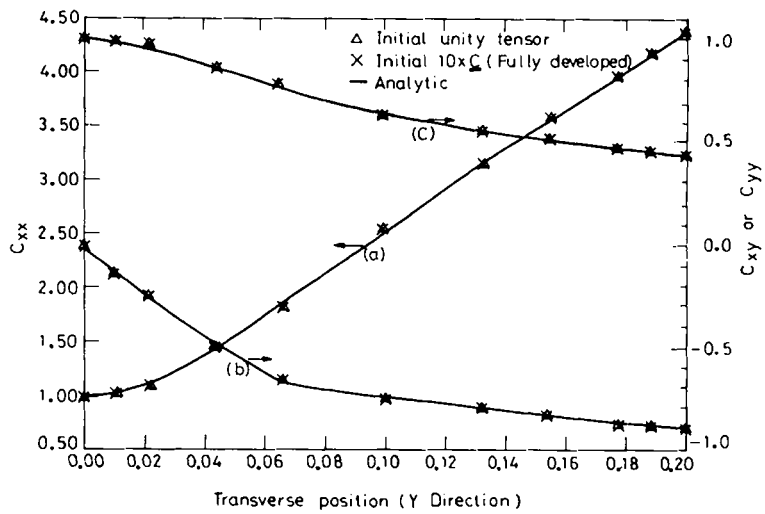

Figure 4. Variation of strain tensor for straight planar flow at outlet of analysed domain: (a) C_{xx}; (b) C_{xy}; (c) C_{yy}

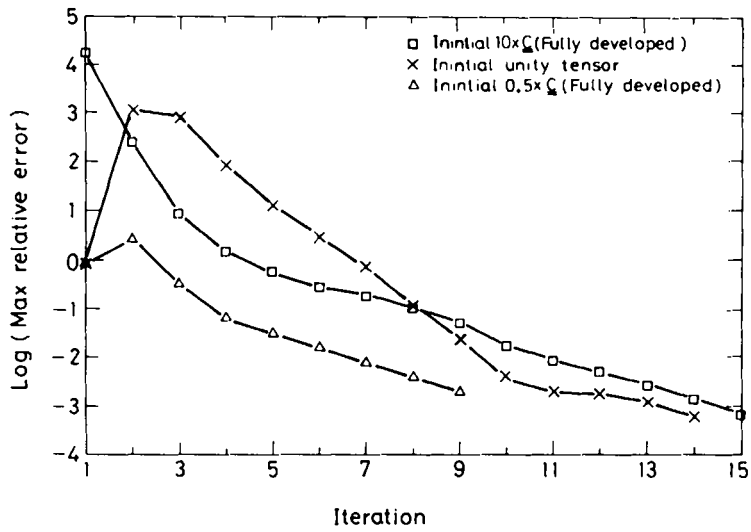

Figure 5. Convergence of C_{xx} for straight planar channel flow (θ = 6·07 s)

field was imposed at the nodal points of the finite element meshes for the strain integrations. Three finite element meshes with increasing resolution in the x-direction were used. The coarsest mesh (mesh A, shown in Figure 3(b)) has only 11 nodal points along a radial line, while mesh B (not shown) has 15 and the finest (mesh C, not shown) has 21. Material entering the region is assumed to be undeformed, so that $\mathbf{C} = \mathbf{I}$. This was also taken as the initial guess for the iterative solution process. The strain field can be calculated analytically by solving the following non-

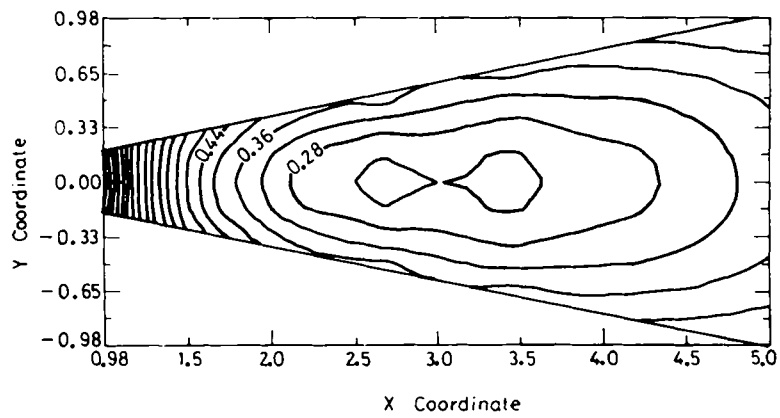

Figure 6. Contour plot of C_{xx} component of C for diverging radial flow (θ = 6·07 s, mesh A)

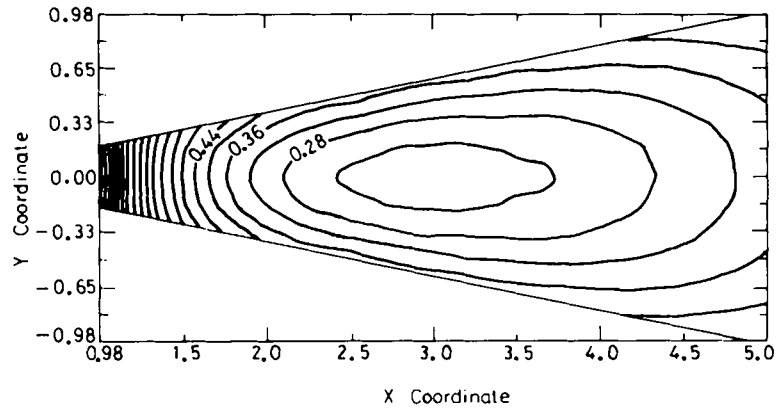

Figure 7. Contour plot of C_{xx} component of C for diverging radial flow (θ = 6·07 s, mesh B)

linear initial value system (the IMSL routine DGEAR was called to solve it):

$$\frac{dC_{11}}{dr} = -\frac{2}{r}C_{11} - \frac{r}{3{\cdot}2\theta}(C_{11}^2 + C_{12}^2 - 1),$$

$$\frac{dC_{12}}{dr} = -\frac{r}{3{\cdot}2\theta}C_{12}(C_{11} + C_{22}), \tag{13}$$

$$\frac{dC_{22}}{dr} = \frac{2}{r}C_{22} - \frac{r}{3{\cdot}2\theta}(C_{12}^2 + C_{22}^2 - 1),$$

subject to $C_{11}(1) = 1$, $C_{12}(1) = 0$, $C_{22}(1) = 1$.

Here the velocity is assumed to be

$$u_r = 1{\cdot}6/r.$$

The material properties, e.g. relaxation time θ_K, were taken to be the same as those for the first test problem. For the following definition of the Weissengberg number,

$$We = \theta u_0 / r_0,$$

we have $We = 9{\cdot}71$ and $0{\cdot}75$ for the two modes respectively.

It should be noted that C_{11}, C_{12} and C_{22} in equations (13) are components of the strain tensor in the cylindrical co-ordinate system, and their solutions must be further transformed to the corresponding components in the Cartesian rectangular co-ordinate system for subsequent comparison. Contour plots of the C_{xx}, C_{xy} and C_{yy} components for the FEM and analytical solutions are shown in Figures 6–10. There are significant oscillations in the C_{xx} component for the coarsest mesh. The results for the finest mesh show excellent agreement between FEM and analytic solutions. The simulated results are also compared with the analytic solutions in Figures 11–13 for two streamlines. One path is near the upper boundary and the second is along the x-

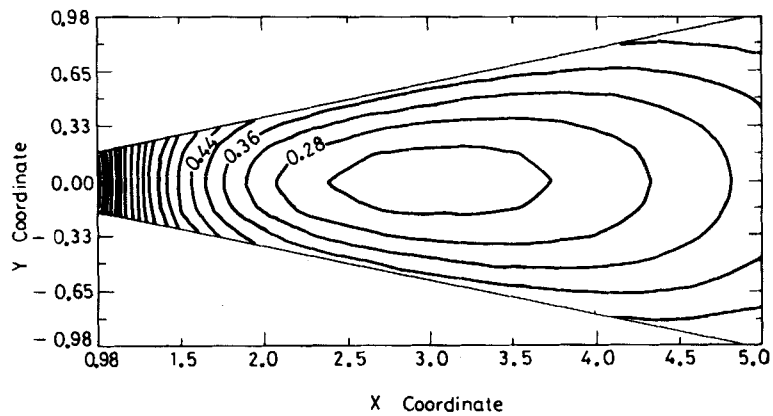

Figure 8. Contour plot of C_{xx} component of C for diverging radial flow ($\theta = 6{\cdot}07$ s, mesh C or analytic solution)

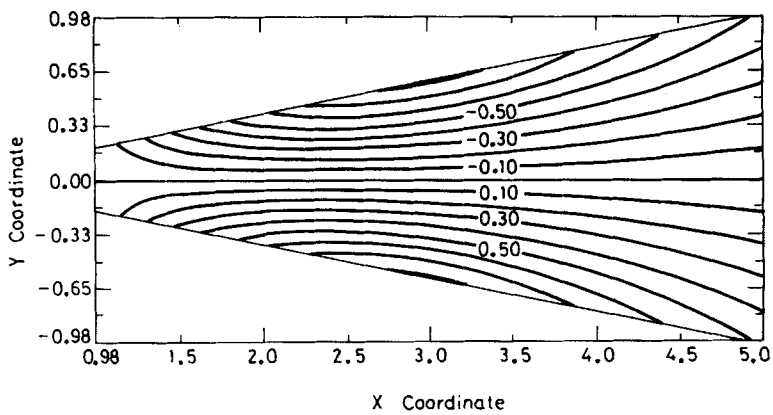

Figure 9. Contour plot of C_{xy} component of C for diverging radial flow ($\theta = 6{\cdot}07$ s, mesh C or analytic solution)

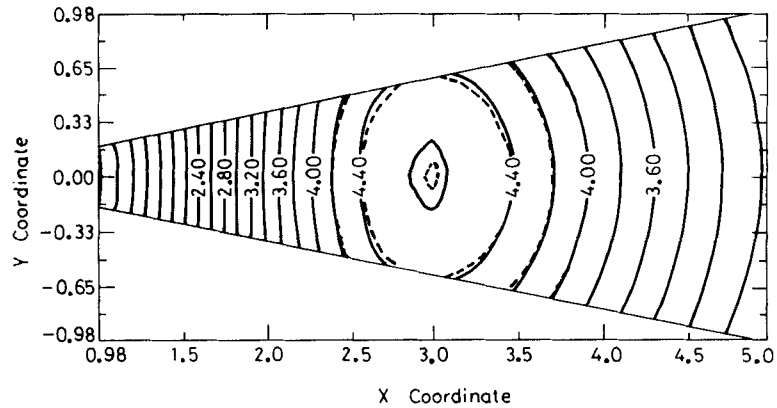

Figure 10. Contour plot of C_{yy} component of C for diverging radial flow: solid line, analytic solution; dashed line, FEM for mesh C (θ = 6·07 s)

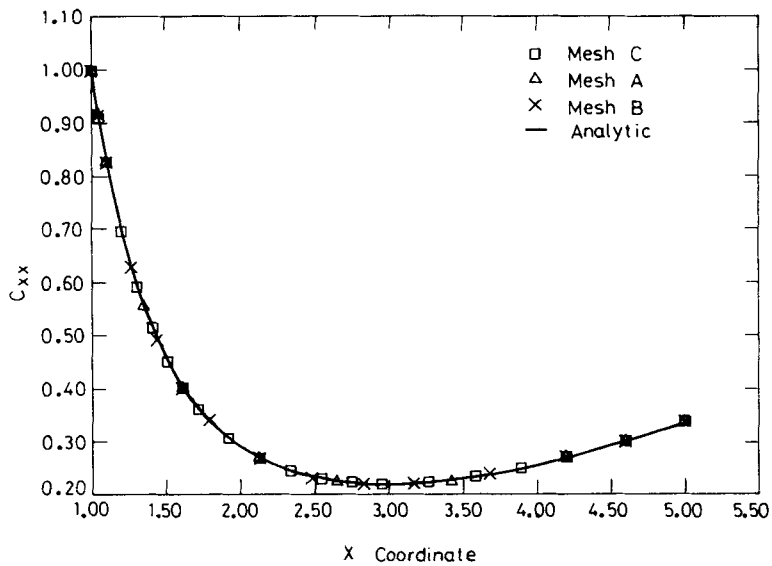

Figure 11. Variation of C_{xx} along centreline for diverging radial flow (θ = 6·07 s)

axis, as shown in Figure 3(b). As expected from the contour plots, the distribution of C_{xx} for the coarsest mesh is inaccurate and shows some oscillatory behaviour. The maximal relative error based on the analytic solutions found in Figure 13 (curve(b)) for C_{yy} at the top streamline is only 1.8%. Figure 14 shows the convergence of the numerical scheme for the radial flow in the case where the unity strain tensor was taken as the initial guess.

To test the robustness of our algorithm, numerical calculations were carried out with revised finite element meshes as shown in Figure 15, in which the mesh lines do not lie along the streamlines, just like in most situations of numerical flow simulation of viscoelastic fluids. Figures 16(a) and 16(b) show good agreement between the analytic and numerical solutions with the

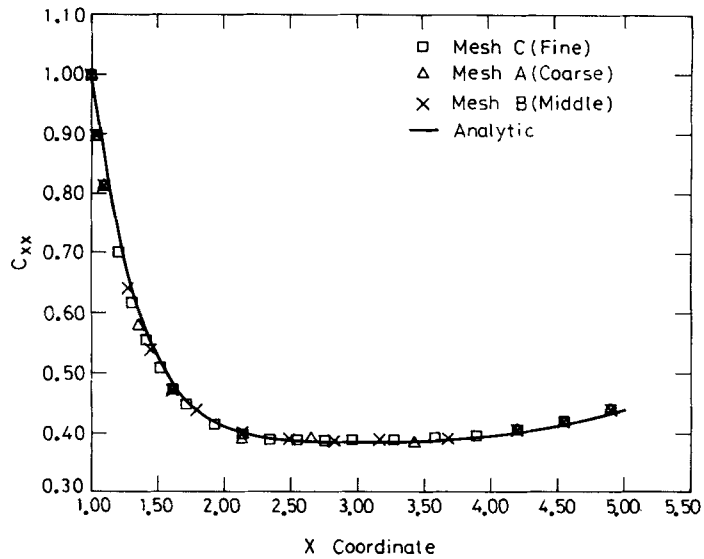

Figure 12. Variation of C_{xx} along top streamline for diverging radial flow (θ = 6·07 s)

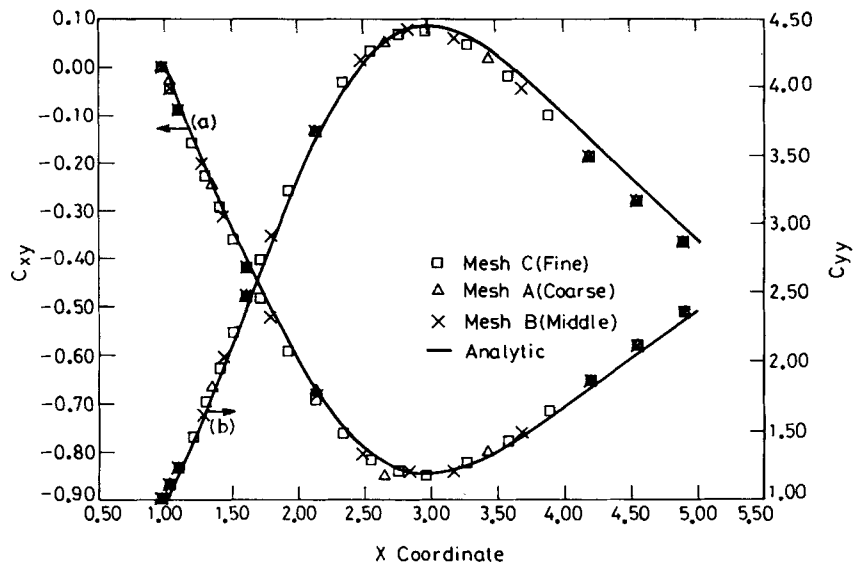

Figure 13. Variation of (a) C_{xy} and (b) C_{yy} along top streamline for diverging radial flow (θ = 6·07 s)

revised meshes. In both cases the unity matrix was prescribed as the initial guess for the elastic strain tensor **C** and convergence was achieved within 30 iterations.

CONCLUSIONS

We have shown an efficient finite element technique which should prove useful in the analysis of flows of Leonov fluids. The culmination of this technique is the ability to calculate the stress field

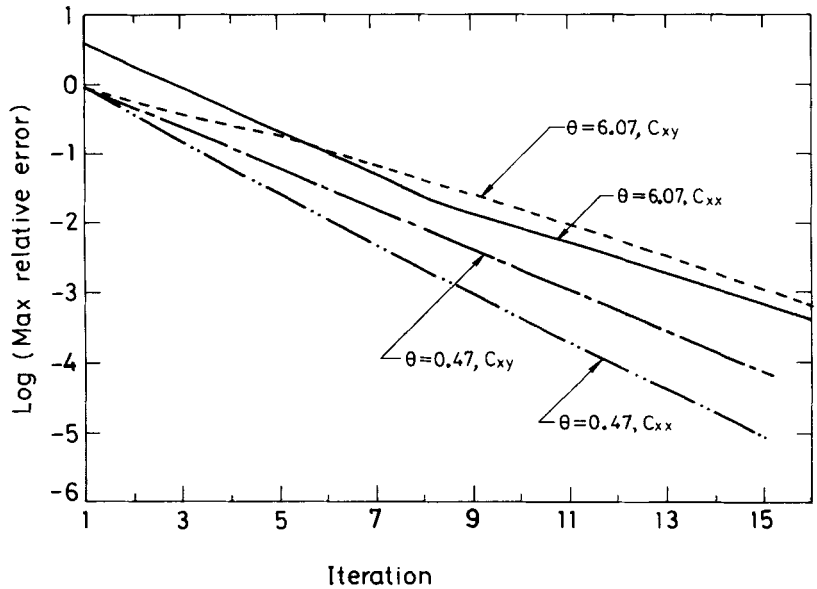

Figure 14. Convergence of proposed numerical scheme for strain calculation for radial flow (unity strain tensor chosen as initial guess for whole domain)

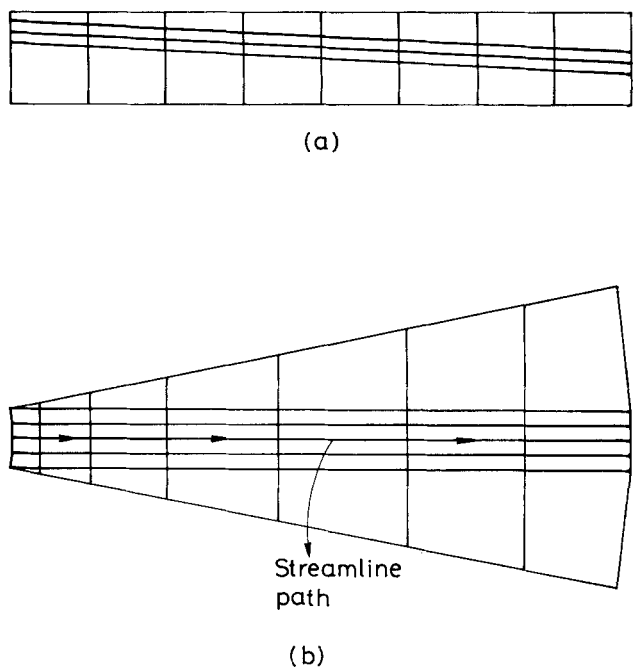

Figure 15. Revised finite element meshes for (a) the straight planar flow and (b) the diverging radial flow

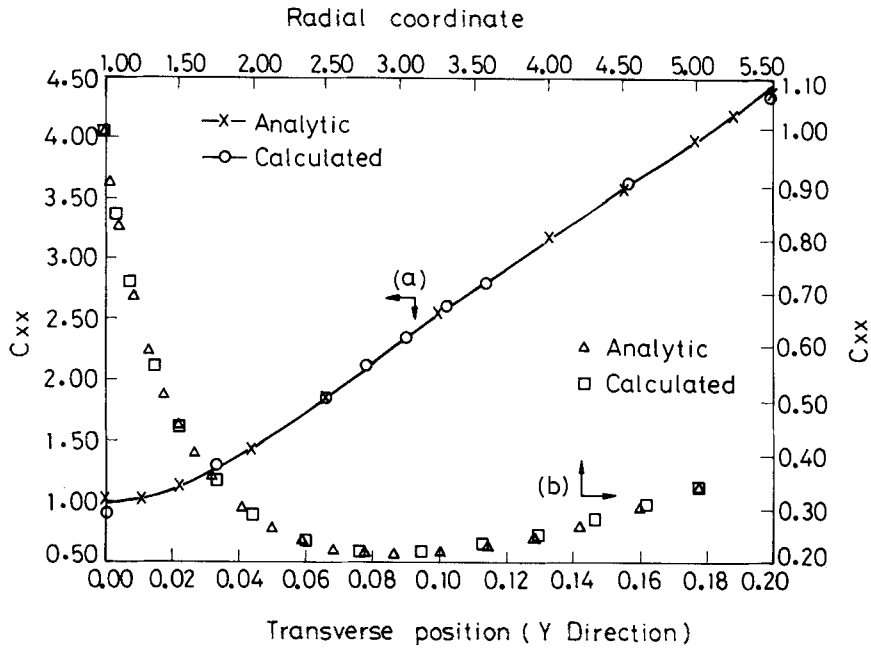

Figure 16. Comparison of the analytic and numerical solutions of C_{xx} with revised finite element mesh being used, (a) C_{xx} at the exit of the straight planar flow, (b) C_{xx} along the centre streamline path of the diverging radial flow

associated with a given flow field for a wide range of differential-type constitutive equations. Continued research is being conducted to develop methods for the numerical simulation of viscoelastic fluid (particularly of the Leonov model) flow with complex geometry in which the velocity field is not known *a priori* and an iterative procedure is needed.

ACKNOWLEDGEMENTS

This work has been supported by the National Science Council, R. O. C., under Grant No. NSC77-0405-E011-04. The useful comments on the treatment of the elastic strain for the Leonov model given by Dr. C. A. Hieber of Cornell University are also greatly appreciated.

REFERENCES

1. M. J. Crochet and R. Keunings, 'Die swell of a Maxwell fluid: numerical prediction', *J. Non-Newtonian Fluid Mech.*, **7**, 199–212 (1980).
2. M. J. Crochet and R. Keunings, 'On numerical die swell calculation', *J. Non-Newtonian Fluid Mech.*, **10**, 85–94 (1982).
3. C. J. Coleman, 'A finite element routine for analysing non-Newtonian flows. Part I: Basic method and preliminary results', *J. Non-Newtonian Fluid Mech.*, **7**, 289–301 (1980).
4. M. Viryayuthakorn and B. Caswell, 'Finite element simulation of viscoelastic flow', *J. Non-Newtonian Fluid Mech.*, **6**, 245–267 (1980).
5. M. J. Crochet and M. Bezy, 'Numerical solution for the flow of viscoelastic fluids', *J. Non-Newtonian Fluid Mech.*, **5**, 201–218 (1979).
6. P. W. Yeh, 'Finite element simulation of viscoelastic fluid flow through a sudden contraction', *Ph.D Thesis*, Massachusetts Institute of Technology, 1984.
7. E. Mitsoulis, 'Finite element analysis of two-dimensional polymer melt flows', *Ph.D. Thesis*, McMaster University, 1984.
8. M. G. N. Perera and K. Strauss, 'Direct numerical solutions of the equations for viscoelastic fluid flow', *J. Non-Newtonian Fluid Mech.*, **5**, 269–283 (1979).

9. R. Keunings, 'On the high Weissenberg number problem', *J. Non-Newtonian Fluid Mech.*, **20**, 209–226 (1986).
10. S. A. White, A. D. Gotsis and D. G. Baird, 'Review of the entry flow problem: experimental and numerical', *J. Non-Newtonian Fluid Mech.*, **24**, 121–160 (1987).
11. M. J. Crochet, A. R. Davies and K. Walters, *Numerical Simulation of Non-Newtonian Flow*, Elsevier Science Publishers B. V., Amsterdam, 1984.
12. A. I. Leonov, 'Non-equilibrium thermodynamics and rheology of viscoelastic polymer media', *Rheol. Acta*, **15**, 85–98 (1976).
13. A. I. Leonov, E. H. Lipkina, E. D. Paskhin and A. N. Prokunin, 'Theoretical and experimental investigation of shearing in elastic polymer liquids', *Rheol. Acta*, **15**, 411–426 (1976).
14. S. F. Shen, 'Simulation of polymeric flows in the injection moulding process', *Int. j. numer. methods fluids*, **4**, 171–183 (1984).
15. R. K. Upadhyay and A. I. Isayev, 'Simulation of two-dimensional planar flow of a viscoelastic fluid', *Rheol. Acta*, **25**, 80–94 (1986).
16. A. I. Isayev and C. A. Hieber, 'Oscillatory shear flow of polymeric systems', *J. Polym. Sci., Polym. Phys. Ed.*, **20**, 423–440 (1982).
17. R. K. Upadhyay, A. I. Isayev and S. F. Shen, 'Transient shear flow behavior of polymeric fluids according to the Leonov model', *Rheol. Acta*, **20**, 443–457 (1981).
18. A. I. Isayev and C. A. Hieber, 'Toward a viscoelastic modelling of the injection molding of polymers', *Rheol. Acta*, **19**, 168–182 (1980).
19. E. G. Thompson, J. F. T. Pittman and O. C. Zienkiewicz, 'Some integration techniques for the analysis of viscoelastic flows', *Int. j. numer. methods fluids*, **3**, 165–177 (1983).
20. D. K. Gartling, 'Finite Element Methods for Non-Newtonian Flows', *Sandia Report*, *Sand*85-1704, 1986, p. 57.
21. A. I. Isayev, C. A. Hieber, R. K. Upadhyay and S. F. Shen, 'Time-dependent rheological behavior of polymer system', in G. Astarita, G. Marracci and L. Nicolais (eds), *Rheology, Vol. 3*, Plenum, New York, 1980, pp. 91–98.
22. K. K. Wang, S. F. Shen, C. Cohen, C. A. Hieber and A. I. Isayev, *Progress Report, Computer-Aided Injection Molding System, No. 8*, Cornell University, 1981, p. 87.
23. A. Agrawal and P. R. Dawson, 'A comparison of Galerkin and streamline techniques for integrating strains from an Eulerian flow field', *Int. j. numer. methods eng.*, **21**, 853–881 (1985).